Inventory Efficiency Ratio and the Cross Section of Stock Returns

I. M. Harking

December 1, 2024

Abstract

This paper studies the asset pricing implications of Inventory Efficiency Ratio (IER), and its robustness in predicting returns in the cross-section of equities using the protocol proposed by Novy-Marx and Velikov (2023). A value-weighted long/short trading strategy based on IER achieves an annualized gross (net) Sharpe ratio of 0.64 (0.57), and monthly average abnormal gross (net) return relative to the Fama and French (2015) five-factor model plus a momentum factor of 20 (20) bps/month with a t-statistic of 2.72 (2.81), respectively. Its gross monthly alpha relative to these six factors plus the six most closely related strategies from the factor zoo (Share issuance (1 year), Growth in book equity, Net Payout Yield, Share issuance (5 year), Change in equity to assets, Asset growth) is 16 bps/month with a t-statistic of 2.39.

1 Introduction

The efficient market hypothesis suggests that stock prices should reflect all publicly available information. However, a growing body of literature documents persistent patterns in stock returns that appear to contradict market efficiency (Harvey et al., 2016). These patterns, often called anomalies, raise important questions about market efficiency and asset pricing. One crucial yet underexplored source of information lies in firms' operational efficiency metrics, particularly in how companies manage their working capital.

While extensive research has examined various accounting-based predictors of stock returns, including accruals (Sloan, 1996) and asset growth (Cooper et al., 2008), the predictive power of inventory management efficiency remains relatively unexplored. This gap is particularly notable given that inventory management directly impacts firms' operational performance and cash flows.

We propose that the Inventory Efficiency Ratio (IER) contains valuable information about future stock returns through several economic channels. First, efficient inventory management reduces working capital requirements and improves cash flow generation (Chen et al., 2005). Companies that optimize their inventory levels can deploy capital more productively, potentially leading to higher future profitability and returns.

Second, superior inventory management may signal management quality and operational excellence (Alan et al., 2014). Firms with better inventory management likely have more sophisticated operational systems and more capable management teams, characteristics associated with better future performance. This aligns with (Hirshleifer and Teoh, 2003)'s argument that investors often underreact to signals of operational efficiency.

Third, inventory efficiency improvements can create competitive advantages through reduced storage costs, lower obsolescence risk, and improved customer service (**?**).

These advantages may not be immediately reflected in stock prices due to investors' limited attention to operational metrics, creating predictable patterns in returns.

Our empirical analysis reveals strong evidence that IER predicts cross-sectional stock returns. A value-weighted long/short trading strategy based on IER achieves an annualized gross Sharpe ratio of 0.64, with monthly average abnormal returns of 20 basis points relative to the Fama-French five-factor model plus momentum (t-statistic = 2.72). The strategy's performance remains robust after controlling for transaction costs, with a net Sharpe ratio of 0.57.

Importantly, the predictive power of IER persists among large-cap stocks, with the strategy generating monthly returns of 28 basis points (t-statistic = 3.05) among stocks above the 80th NYSE size percentile. This suggests that the effect is not limited to small, illiquid stocks where trading costs might prohibit implementation.

The signal's economic significance is further demonstrated by its performance relative to other documented anomalies. IER's gross (net) Sharpe ratio exceeds 97% (99%) of previously documented anomalies, and its alpha remains significant even after controlling for the six most closely related anomalies (16 bps/month, t-statistic = 2.39).

Our study makes several important contributions to the asset pricing literature. First, we extend the literature on accounting-based return predictors (Sloan, 1996; Titman et al., 2004) by identifying a novel signal based on operational efficiency. Unlike traditional accounting metrics, IER captures dynamic information about management's operational capabilities.

Second, we contribute to the growing literature on the role of operational metrics in asset pricing (Alan et al., 2014; Chen et al., 2005). Our findings suggest that operational efficiency metrics contain valuable information about future returns that is not fully captured by traditional financial statements or existing factor models.

Finally, our results have important implications for both academic research and investment practice. For researchers, we demonstrate the importance of considering operational metrics in asset pricing models. For practitioners, we identify a robust signal that can enhance portfolio performance, even after accounting for transaction costs and controlling for known factors.

2 Data

Our study examines the predictive power of the Inventory Efficiency Ratio, a financial signal constructed from accounting data to analyze cross-sectional stock returns. We obtain the necessary accounting and financial data from COMPUSTAT, which provides comprehensive firm-level observations for publicly traded companies. To construct our signal, we utilize COMPUSTAT's item CSTK for total common and preferred stock capital, and item COGS for cost of goods sold. Total common and preferred stock capital (CSTK) represents the total par or stated value of outstanding stock, while cost of goods sold (COGS) reflects the direct costs attributable to the production of goods sold by the company. The construction of our signal follows a specific methodology where we calculate the year-over-year change in CSTK (current CSTK minus lagged CSTK) and scale this difference by the lagged value of COGS. This ratio provides insight into how changes in a company's equity capital structure relate to its production costs, potentially capturing aspects of operational efficiency and capital management. We compute this ratio using end-of-fiscal-year values to maintain consistency and comparability across firms and time periods. The scaling by lagged COGS helps to normalize the change in capital structure relative to the firm's operational scale, making the signal more comparable across firms of different sizes.

3 Signal diagnostics

Figure 1 plots descriptive statistics for the IER signal. Panel A plots the time-series of the mean, median, and interquartile range for IER. On average, the cross-sectional mean (median) IER is -0.06 (-0.00) over the 1966 to 2023 sample, where the starting date is determined by the availability of the input IER data. The signal's interquartile range spans -0.01 to 0.00. Panel B of Figure 1 plots the time-series of the coverage of the IER signal for the CRSP universe. On average, the IER signal is available for 6.54% of CRSP names, which on average make up 7.95% of total market capitalization.

4 Does IER predict returns?

Table 1 reports the performance of portfolios constructed using a value-weighted, quintile sort on IER using NYSE breaks. The first two lines of Panel A report monthly average excess returns for each of the five portfolios and for the long/short portfolio that buys the high IER portfolio and sells the low IER portfolio. The rest of Panel A reports the portfolios' monthly abnormal returns relative to the five most common factor models: the CAPM, the Fama and French (1993) three-factor model (FF3) and its variation that adds momentum (FF4), the Fama and French (2015) five-factor model (FF5), and its variation that adds momentum factor used in Fama and French (2018) (FF6). The table shows that the long/short IER strategy earns an average return of 0.36% per month with a t-statistic of 4.84. The annualized Sharpe ratio of the strategy is 0.64. The alphas range from 0.20% to 0.38% per month and have t-statistics exceeding 2.72 everywhere. The lowest alpha is with respect to the FF6 factor model.

Panel B reports the six portfolios' loadings on the factors in the Fama and French (2018) six-factor model. The long/short strategy's most significant loading is 0.30, with a t-statistic of 6.16 on the CMA factor. Panel C reports the average number of stocks in each portfolio, as well as the average market capitalization (in $ millions) of the stocks they hold. In an average month, the five portfolios have at least 569 stocks and an average market capitalization of at least $1,391 million.

Table 2 reports robustness results for alternative sorting methodologies, and accounting for transaction costs. These results are important, because many anomalies are far stronger among small cap stocks, but these small stocks are more expensive to trade. Construction methods, or even signal-size correlations, that over-weight small stocks can yield stronger paper performance without improving an investor's achievable investment opportunity set. Panel A reports gross returns and alphas for the long/short strategies made using various different protfolio constructions. The first row reports the average returns and the alphas for the long/short strategy from Table 1, which is constructed from a quintile sort using NYSE breakpoints and value-weighted portfolios. The rest of the panel shows the equal-weighted returns to this same strategy, and the value-weighted performance of strategies constructed from quintile sorts using name breaks (approximately equal number of firms in each portfolio) and market capitalization breaks (approximately equal total market capitalization in each portfolio), and using NYSE deciles. The average return is lowest for the quintile sort using cap breakpoints and value-weighted portfolios, and equals 31 bps/month with a t-statistics of 4.09. Out of the twenty-five alphas reported in Panel A, the t-statistics for twenty-five exceed two, and for nineteen exceed three.

Panel B reports for these same strategies the average monthly net returns and the generalized net alphas of Novy-Marx and Velikov (2016). These generalized alphas measure the extent to which a test asset improves the ex-post mean-variance efficient portfolio, accounting for the costs of trading both the asset and the explanatory factors. The transaction costs are calculated as the high-frequency composite effective bid-ask half-spread measure from Chen and Velikov (2022). The net average returns reported in the first column range between 28-36bps/month. The lowest return, (28 bps/month), is achieved from the quintile sort using cap breakpoints and value-weighted portfolios, and has an associated t-statistic of 3.63. Out of the twenty-five construction-methodology-factor-model pairs reported in Panel B, the IER trading strategy improves the achievable mean-variance efficient frontier spanned by the factor models in twenty-five cases, and significantly expands the achievable frontier in twenty-five cases.

Table 3 provides direct tests for the role size plays in the IER strategy performance. Panel A reports the average returns for the twenty-five portfolios constructed from a conditional double sort on size and IER, as well as average returns and alphas for long/short trading IER strategies within each size quintile. Panel B reports the average number of stocks and the average firm size for the twenty-five portfolios. Among the largest stocks (those with market capitalization greater than the 80^{th} NYSE percentile), the IER strategy achieves an average return of 28 bps/month with a t-statistic of 3.05. Among these large cap stocks, the alphas for the IER strategy relative to the five most common factor models range from 19 to 27 bps/month with t-statistics between 2.02 and 2.90.

5 How does IER perform relative to the zoo?

Figure 2 puts the performance of IER in context, showing the long/short strategy performance relative to other strategies in the "factor zoo." It shows Sharpe ratio histograms, both for gross and net returns (Panel A and B, respectively), for 212 documented anomalies in the zoo.[1] The vertical red line shows where the Sharpe ratio for the IER strategy falls in the distribution. The IER strategy's gross (net) Sharpe ratio of 0.64 (0.57) is greater than 97% (99%) of anomaly Sharpe ratios,

[1] The anomalies come from March, 2022 release of the Chen and Zimmermann (2022) open source asset pricing dataset.

respectively.

Figure 3 plots the growth of a \$1 invested in these same 212 anomaly trading strategies (gray lines), and compares those with the growth of a \$1 invested in the IER strategy (red line).[2] Ignoring trading costs, a \$1 invested in the IER strategy would have yielded \$9.64 which ranks the IER strategy in the top 1% across the 212 anomalies. Accounting for trading costs, a \$1 invested in the IER strategy would have yielded \$7.33 which ranks the IER strategy in the top 0% across the 212 anomalies.

Figure 4 plots percentile ranks for the 212 anomaly trading strategies in terms of gross and Novy-Marx and Velikov (2016) net generalized alphas with respect to the CAPM, and the Fama-French three-, four-, five-, and six-factor models from Table 1, and indicates the ranking of the IER relative to those. Panel A shows that the IER strategy gross alphas fall between the 66 and 74 percentiles across the five factor models. Panel B shows that, accounting for trading costs, a large fraction of anomalies have not improved the investment opportunity set of an investor with access to the factor models over the 196606 to 202306 sample. For example, 45% (53%) of the 212 anomalies would not have improved the investment opportunity set for an investor having access to the Fama-French three-factor (six-factor) model. The IER strategy has a positive net generalized alpha for five out of the five factor models. In these cases IER ranks between the 85 and 90 percentiles in terms of how much it could have expanded the achievable investment frontier.

6 Does IER add relative to related anomalies?

With so many anomalies, it is possible that any proposed, new cross-sectional predictor is just capturing some combination of known predictors. It is consequently

[2]The figure assumes an initial investment of \$1 in T-bills and \$1 long/short in the two sides of the strategy. Returns are compounded each month, assuming, as in Detzel et al. (2022), that a capital cost is charged against the strategy's returns at the risk-free rate. This excess return corresponds more closely to the strategy's economic profitability.

natural to investigate to what extent the proposed predictor adds additional predictive power beyond the most closely related anomalies. Closely related anomalies are more likely to be formed on the basis of signals with higher absolute correlations. Figure 5 plots a name histogram of the correlations of IER with 210 filtered anomaly signals.[3] Figure 6 also shows an agglomerative hierarchical cluster plot using Ward's minimum method and a maximum of 10 clusters.

A closely related anomaly is also more likely to price IER or at least to weaken the power IER has predicting the cross-section of returns. Figure 7 plots histograms of t-statistics for predictability tests of IER conditioning on each of the 210 filtered anomaly signals one at a time. Panel A reports t-statistics on β_{IER} from Fama-MacBeth regressions of the form $r_{i,t} = \alpha + \beta_{IER} IER_{i,t} + \beta_X X_{i,t} + \epsilon_{i,t}$, where X stands for one of the 210 filtered anomaly signals at a time. Panel B plots t-statistics on α from spanning tests of the form: $r_{IER,t} = \alpha + \beta r_{X,t} + \epsilon_t$, where $r_{X,t}$ stands for the returns to one of the 210 filtered anomaly trading strategies at a time. The strategies employed in the spanning tests are constructed using quintile sorts, value-weighting, and NYSE breakpoints. Panel C plots t-statistics on the average returns to strategies constructed by conditional double sorts. In each month, we sort stocks into quintiles based one of the 210 filtered anomaly signals. Then, within each quintile, we sort stocks into quintiles based on IER. Stocks are finally grouped into five IER portfolios by combining stocks within each anomaly sorting portfolio. The panel plots the t-statistics on the average returns of these conditional double-sorted IER trading strategies conditioned on each of the 210 filtered anomalies.

Table 4 reports Fama-MacBeth cross-sectional regressions of returns on IER and the six anomalies most closely-related to it. The six most-closely related anomalies

[3] When performing tests at the underlying signal level (e.g., the correlations plotted in Figure 5), we filter the 212 anomalies to avoid small sample issues. For each anomaly, we calculate the common stock observations in an average month for which both the anomaly and the test signal are available. In the filtered anomaly set, we drop anomalies with fewer than 100 common stock observations in an average month.

are picked as those with the highest combined rank where the ranks are based on the absolute value of the Spearman correlations in Panel B of Figure 5 and the R^2 from the spanning tests in Figure 7, Panel B. Controlling for each of these signals at a time, the t-statistics on the IER signal in these Fama-MacBeth regressions exceed 3.76, with the minimum t-statistic occurring when controlling for Net Payout Yield. Controlling for all six closely related anomalies, the t-statistic on IER is 2.85.

Similarly, Table 5 reports results from spanning tests that regress returns to the IER strategy onto the returns of the six most closely-related anomalies and the six Fama-French factors. Controlling for the six most-closely related anomalies individually, the IER strategy earns alphas that range from 17-22bps/month. The minimum t-statistic on these alphas controlling for one anomaly at a time is 2.38, which is achieved when controlling for Net Payout Yield. Controlling for all six closely-related anomalies and the six Fama-French factors simultaneously, the IER trading strategy achieves an alpha of 16bps/month with a t-statistic of 2.39.

7 Does IER add relative to the whole zoo?

Finally, we can ask how much adding IER to the entire factor zoo could improve investment performance. Figure 8 plots the growth of $1 invested in trading strategies that combine multiple anomalies following Chen and Velikov (2022). The combinations use either the 155 anomalies from the zoo that satisfy our inclusion criteria (blue lines) or these 155 anomalies augmented with the IER signal.[4] We consider one different methods for combining signals.

Panel A shows results using "Average rank" as the combination method. This method sorts stocks on the basis of forecast excess returns, where these are calculated on the basis of their average cross-sectional percentile rank across return predictors,

[4] We filter the 207 Chen and Zimmermann (2022) anomalies and require for each anomaly the average month to have at least 40% of the cross-sectional observations available for market capitalization on CRSP in the period for which IER is available.

and the predictors are all signed so that higher ranks are associated with higher average returns. For this method, \$1 investment in the 155-anomaly combination strategy grows to \$2333.55, while \$1 investment in the combination strategy that includes IER grows to \$2377.67.

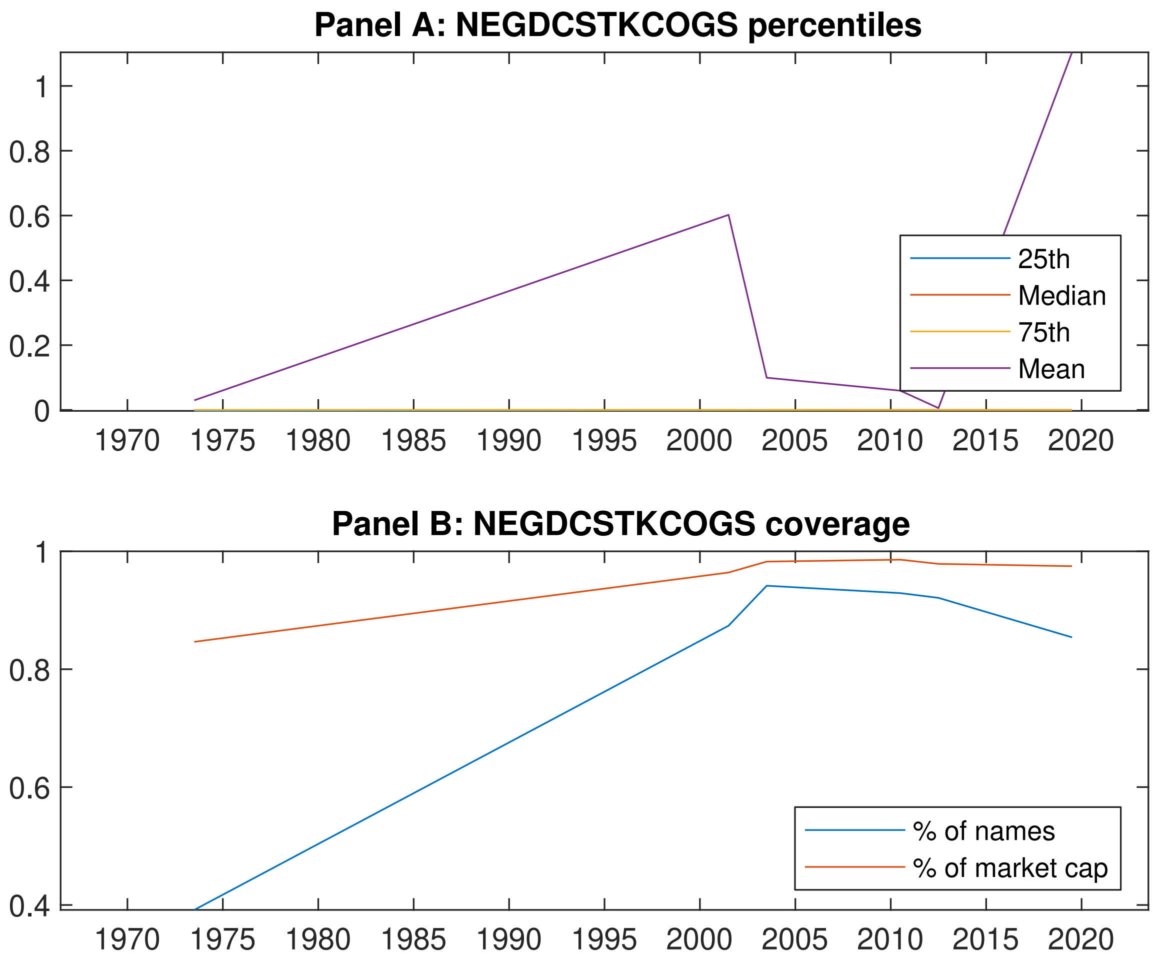

Figure 1: Times series of IER percentiles and coverage.
This figure plots descriptive statistics for IER. Panel A shows cross-sectional percentiles of IER over the sample. Panel B plots the monthly coverage of IER relative to the universe of CRSP stocks with available market capitalizations.

Table 1: Basic sort: VW, quintile, NYSE-breaks

This table reports average excess returns and alphas for portfolios sorted on IER. At the end of each month, we sort stocks into five portfolios based on their signal using NYSE breakpoints. Panel A reports average value-weighted quintile portfolio (L,2,3,4,H) returns in excess of the risk-free rate, the long-short extreme quintile portfolio (H-L) return, and alphas with respect to the CAPM, Fama and French (1993) three-factor model, Fama and French (1993) three-factor model augmented with the Carhart (1997) momentum factor, Fama and French (2015) five-factor model, and the Fama and French (2015) five-factor model augmented with the Carhart (1997) momentum factor following Fama and French (2018). Panel B reports the factor loadings for the quintile portfolios and long-short extreme quintile portfolio in the Fama and French (2015) five-factor model. Panel C reports the average number of stocks and market capitalization of each portfolio. T-statistics are in brackets. The sample period is 196606 to 202306.

Panel A: Excess returns and alphas on IER-sorted portfolios						
	(L)	(2)	(3)	(4)	(H)	(H-L)
r^e	0.41	0.54	0.68	0.67	0.76	0.36
	[2.33]	[2.82]	[3.54]	[3.98]	[4.53]	[4.84]
α_{CAPM}	-0.14	-0.07	0.08	0.15	0.24	0.38
	[-2.95]	[-1.43]	[1.47]	[3.04]	[5.10]	[5.08]
α_{FF3}	-0.14	-0.06	0.09	0.10	0.19	0.33
	[-2.93]	[-1.25]	[1.71]	[2.38]	[4.41]	[4.49]
α_{FF4}	-0.12	-0.02	0.11	0.07	0.17	0.29
	[-2.50]	[-0.50]	[1.96]	[1.59]	[3.93]	[3.94]
α_{FF5}	-0.13	-0.00	0.11	0.00	0.09	0.22
	[-2.65]	[-0.10]	[2.07]	[0.08]	[2.18]	[3.01]
α_{FF6}	-0.12	0.02	0.12	-0.02	0.09	0.20
	[-2.36]	[0.38]	[2.23]	[-0.37]	[2.03]	[2.72]
Panel B: Fama and French (2018) 6-factor model loadings for IER-sorted portfolios						
β_{MKT}	0.96	1.03	1.03	1.00	0.99	0.03
	[83.11]	[94.36]	[78.28]	[99.75]	[99.27]	[1.45]
β_{SMB}	-0.06	0.03	0.07	-0.07	-0.02	0.04
	[-3.34]	[1.64]	[3.52]	[-4.61]	[-1.46]	[1.39]
β_{HML}	0.04	0.02	-0.03	0.07	0.04	-0.00
	[1.76]	[0.80]	[-1.24]	[3.65]	[1.98]	[-0.04]
β_{RMW}	0.03	-0.04	-0.01	0.15	0.13	0.10
	[1.16]	[-1.96]	[-0.46]	[7.41]	[6.63]	[3.01]
β_{CMA}	-0.08	-0.14	-0.06	0.18	0.23	0.30
	[-2.37]	[-4.45]	[-1.71]	[6.42]	[8.02]	[6.16]
β_{UMD}	-0.02	-0.04	-0.02	0.03	0.01	0.03
	[-1.77]	[-3.24]	[-1.22]	[2.99]	[0.88]	[1.68]
Panel C: Average number of firms (n) and market capitalization (me)						
n	807	708	569	693	768	
me ($\$10^6$)	1919	1391	1920	2238	2444	

Table 2: Robustness to sorting methodology & trading costs
This table evaluates the robustness of the choices made in the IER strategy construction methodology. In each panel, the first row shows results from a quintile, value-weighted sort using NYSE break points as employed in Table 1. Each of the subsequent rows deviates in one of the three choices at a time, and the choices are specified in the first three columns. For each strategy construction methodology, the table reports average excess returns and alphas with respect to the CAPM, Fama and French (1993) three-factor model, Fama and French (1993) three-factor model augmented with the Carhart (1997) momentum factor, Fama and French (2015) five-factor model, and the Fama and French (2015) five-factor model augmented with the Carhart (1997) momentum factor following Fama and French (2018). Panel A reports average returns and alphas with no adjustment for trading costs. Panel B reports net average returns and Novy-Marx and Velikov (2016) generalized alphas as prescribed by Detzel et al. (2022). T-statistics are in brackets. The sample period is 196606 to 202306.

Panel A: Gross Returns and Alphas								
Portfolios	Breaks	Weights	r^e	α_{CAPM}	α_{FF3}	α_{FF4}	α_{FF5}	α_{FF6}
Quintile	NYSE	VW	0.36	0.38	0.33	0.29	0.22	0.20
			[4.84]	[5.08]	[4.49]	[3.94]	[3.01]	[2.72]
Quintile	NYSE	EW	0.56	0.62	0.54	0.47	0.38	0.34
			[8.39]	[9.59]	[8.98]	[7.88]	[6.79]	[6.06]
Quintile	Name	VW	0.35	0.36	0.33	0.30	0.25	0.24
			[4.73]	[4.83]	[4.41]	[3.96]	[3.35]	[3.13]
Quintile	Cap	VW	0.31	0.31	0.28	0.24	0.22	0.20
			[4.09]	[4.04]	[3.68]	[3.09]	[2.87]	[2.50]
Decile	NYSE	VW	0.38	0.36	0.31	0.25	0.25	0.20
			[4.02]	[3.85]	[3.37]	[2.62]	[2.59]	[2.10]

Panel B: Net Returns and Novy-Marx and Velikov (2016) generalized alphas								
Portfolios	Breaks	Weights	r^e_{net}	α^*_{CAPM}	α^*_{FF3}	α^*_{FF4}	α^*_{FF5}	α^*_{FF6}
Quintile	NYSE	VW	0.32	0.35	0.30	0.28	0.21	0.20
			[4.36]	[4.65]	[4.15]	[3.87]	[2.95]	[2.81]
Quintile	NYSE	EW	0.36	0.41	0.34	0.30	0.18	0.16
			[4.95]	[5.78]	[5.11]	[4.64]	[2.87]	[2.65]
Quintile	Name	VW	0.32	0.33	0.31	0.29	0.24	0.24
			[4.25]	[4.46]	[4.09]	[3.88]	[3.26]	[3.14]
Quintile	Cap	VW	0.28	0.28	0.25	0.23	0.21	0.19
			[3.63]	[3.65]	[3.33]	[3.03]	[2.73]	[2.53]
Decile	NYSE	VW	0.34	0.33	0.29	0.25	0.23	0.20
			[3.60]	[3.48]	[3.06]	[2.68]	[2.45]	[2.20]

Table 3: Conditional sort on size and IER

This table presents results for conditional double sorts on size and IER. In each month, stocks are first sorted into quintiles based on size using NYSE breakpoints. Then, within each size quintile, stocks are further sorted based on IER. Finally, they are grouped into twenty-five portfolios based on the intersection of the two sorts. Panel A presents the average returns to the 25 portfolios, as well as strategies that go long stocks with high IER and short stocks with low IER .Panel B documents the average number of firms and the average firm size for each portfolio. The sample period is 196606 to 202306.

Panel A: portfolio average returns and time-series regression results

		IER Quintiles					IER Strategies					
		(L)	(2)	(3)	(4)	(H)	r^e	α_{CAPM}	α_{FF3}	α_{FF4}	α_{FF5}	α_{FF6}
Size quintiles	(1)	0.38	0.71	0.92	0.98	0.98	0.60	0.65	0.59	0.55	0.46	0.43
		[1.46]	[2.67]	[3.54]	[3.81]	[4.11]	[7.90]	[8.66]	[8.30]	[7.58]	[6.59]	[6.16]
	(2)	0.51	0.75	0.80	0.89	0.96	0.45	0.50	0.41	0.37	0.29	0.28
		[2.20]	[3.07]	[3.29]	[3.88]	[4.34]	[5.25]	[5.85]	[5.04]	[4.53]	[3.62]	[3.36]
	(3)	0.55	0.64	0.82	0.80	0.94	0.38	0.41	0.36	0.35	0.26	0.25
		[2.63]	[2.81]	[3.61]	[3.75]	[4.64]	[4.95]	[5.30]	[4.70]	[4.45]	[3.31]	[3.26]
	(4)	0.47	0.65	0.79	0.79	0.81	0.34	0.37	0.29	0.27	0.09	0.09
		[2.37]	[3.06]	[3.69]	[3.94]	[4.28]	[4.16]	[4.52]	[3.81]	[3.42]	[1.23]	[1.18]
	(5)	0.43	0.49	0.50	0.56	0.71	0.28	0.27	0.25	0.20	0.22	0.19
		[2.56]	[2.61]	[2.68]	[3.30]	[4.24]	[3.05]	[2.90]	[2.67]	[2.17]	[2.36]	[2.02]

Panel B: Portfolio average number of firms and market capitalization

		IER Quintiles					IER Quintiles				
		Average n					Average market capitalization ($\$10^6$)				
		(L)	(2)	(3)	(4)	(H)	(L)	(2)	(3)	(4)	(H)
Size quintiles	(1)	389	389	388	386	387	32	34	39	29	29
	(2)	111	110	110	110	110	56	56	57	55	56
	(3)	81	80	81	80	81	98	96	97	99	100
	(4)	68	68	68	68	68	206	206	210	215	217
	(5)	62	62	62	62	62	1369	1463	1727	1599	1766

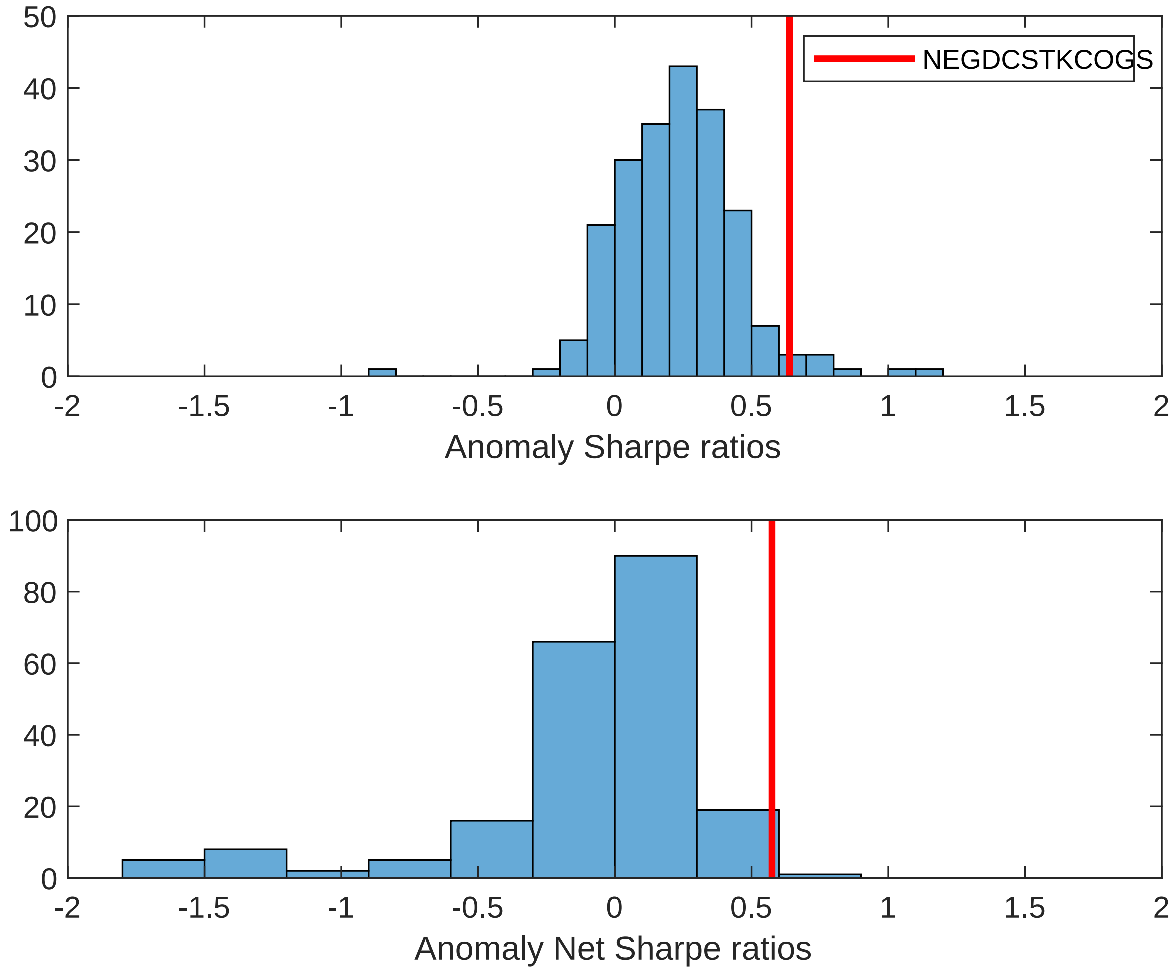

Figure 2: Distribution of Sharpe ratios.
This figure plots a histogram of Sharpe ratios for 212 anomalies, and compares the Sharpe ratio of the IER with them (red vertical line). Panel A plots results for gross Sharpe ratios. Panel B plots results for net Sharpe ratios.

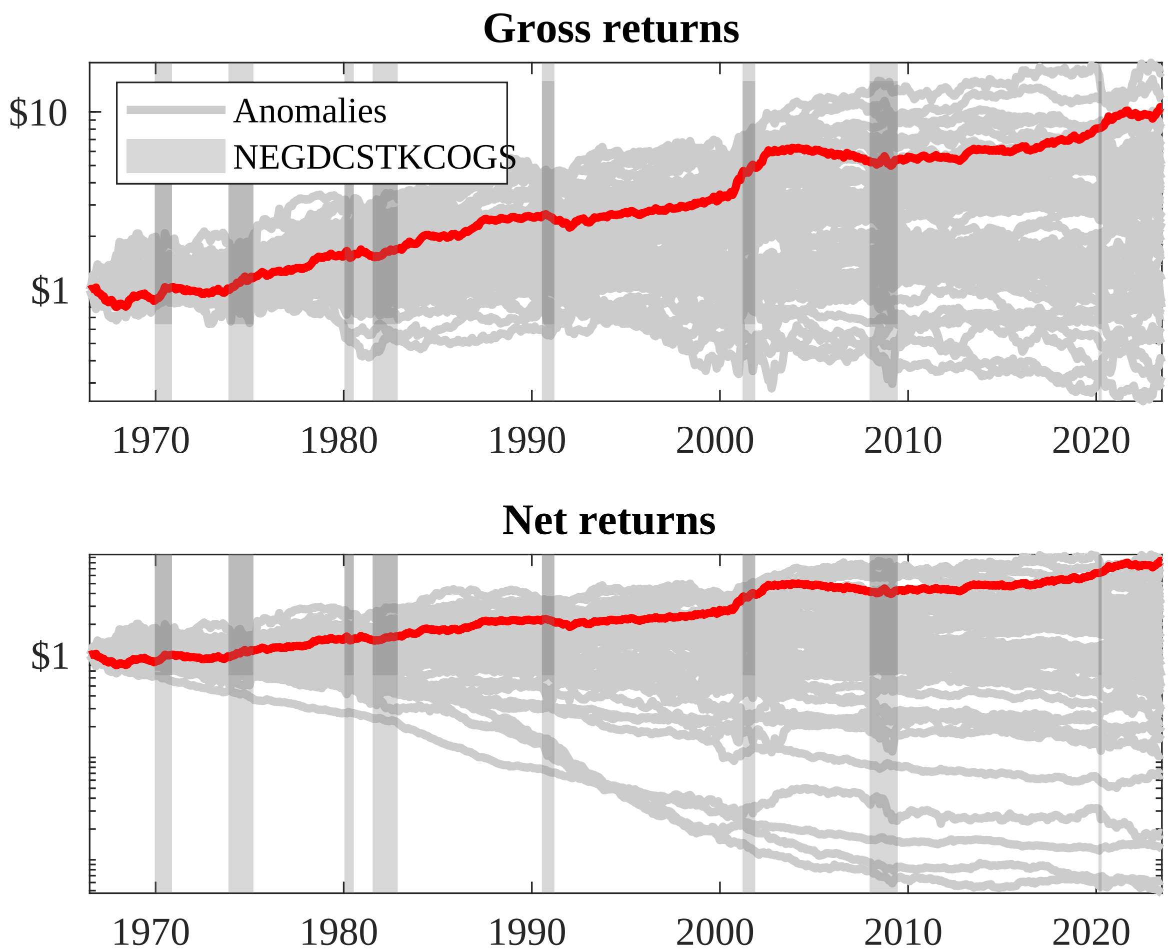

Figure 3: Dollar invested.
This figure plots the growth of a $1 invested in 212 anomaly trading strategies (gray lines), and compares those with the IER trading strategy (red line). The strategies are constructed using value-weighted quintile sorts using NYSE breakpoints. Panel A plots results for gross strategy returns. Panel B plots results for net strtaegy returns.

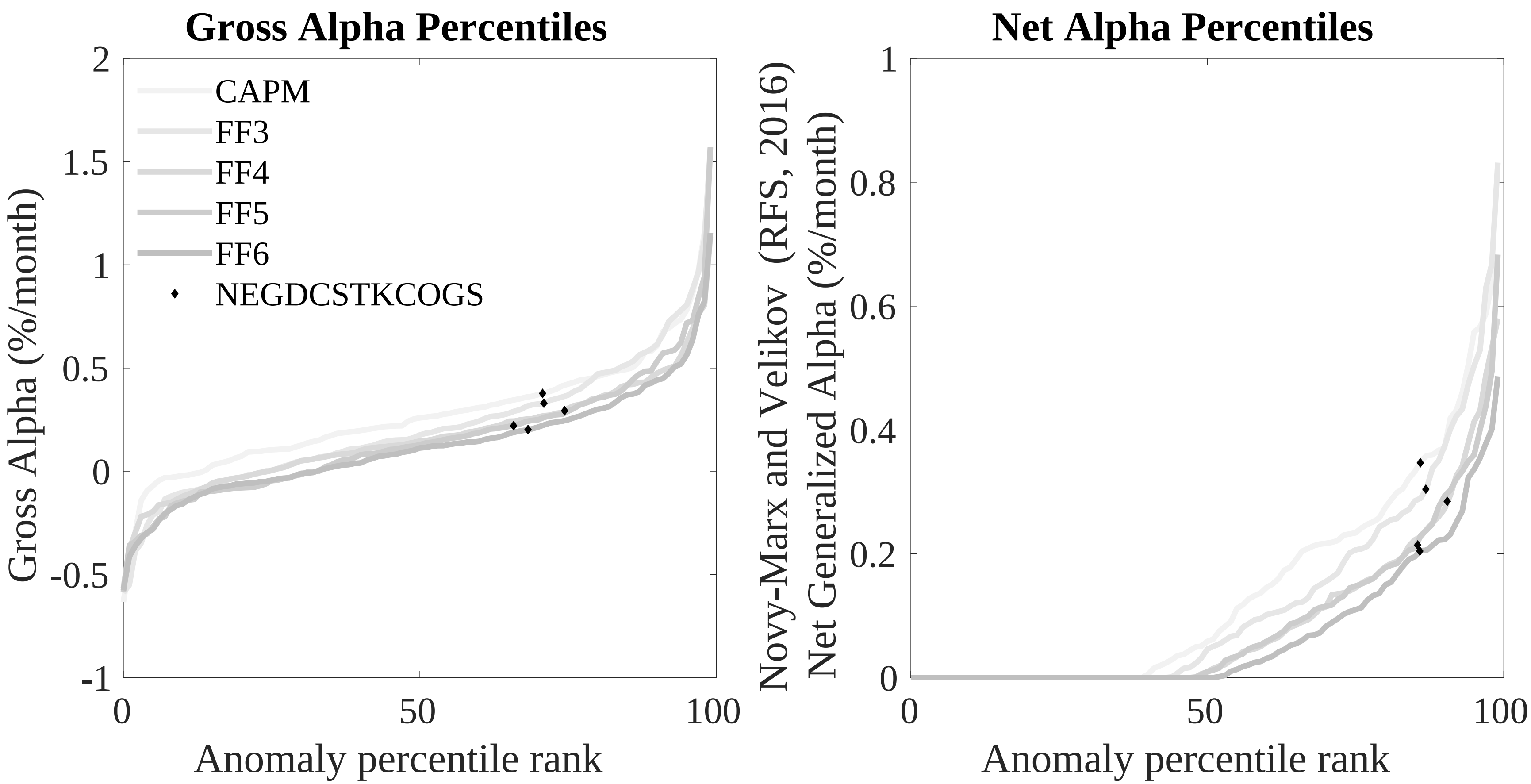

Figure 4: Gross and generalized net alpha percentiles of anomalies relative to factor models
This figure plots the percentile ranks for 212 anomaly trading strategies in terms of alphas (solid lines), and compares those with the IER trading strategy alphas (diamonds). The strategies are constructed using value-weighted quintile sorts using NYSE breakpoints. The alphas include those with respect to the CAPM, Fama and French (1993) three-factor model, Fama and French (1993) three-factor model augmented with the Carhart (1997) momentum factor, Fama and French (2015) five-factor model, and the Fama and French (2015) five-factor model augmented with the Carhart (1997) momentum factor following Fama and French (2018). The left panel plots alphas with no adjustment for trading costs. The right panel plots Novy-Marx and Velikov (2016) net generalized alphas.

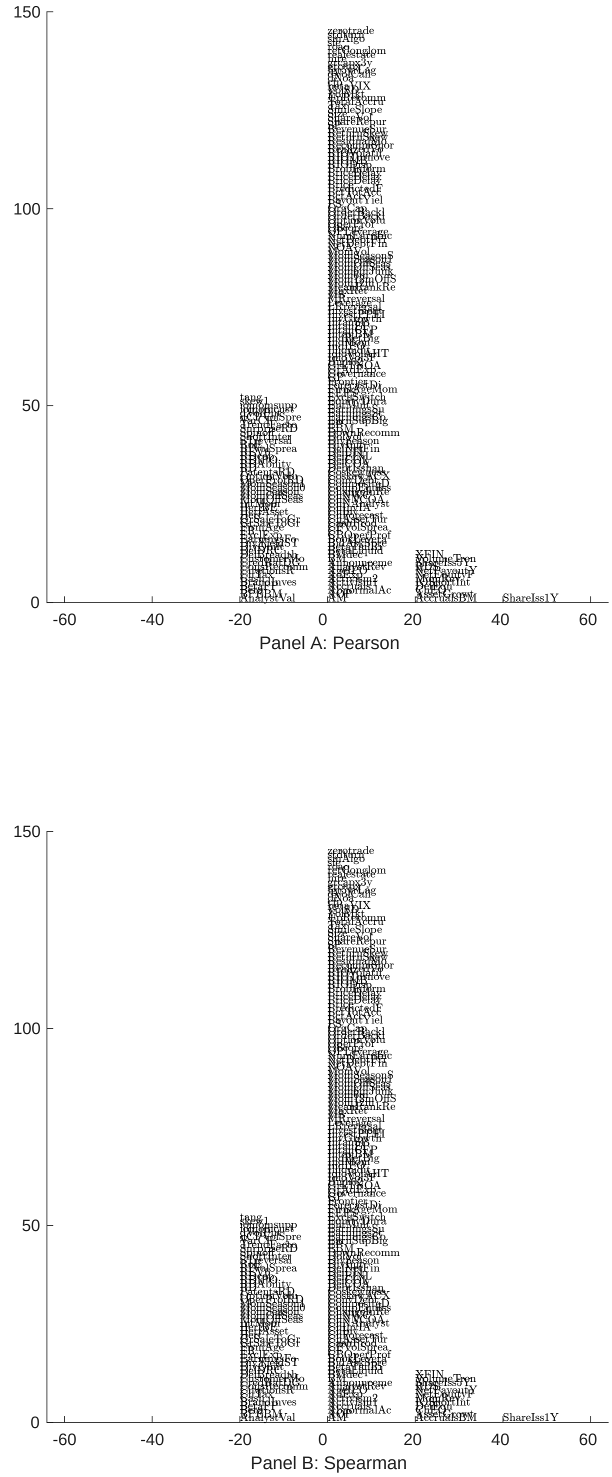

Figure 5: Distribution of correlations.
This figure plots a name histogram of correlations of 210 filtered anomaly signals with IER. The correlations are pooled. Panel A plots Pearson correlations, while Panel B plots Spearman rank correlations.

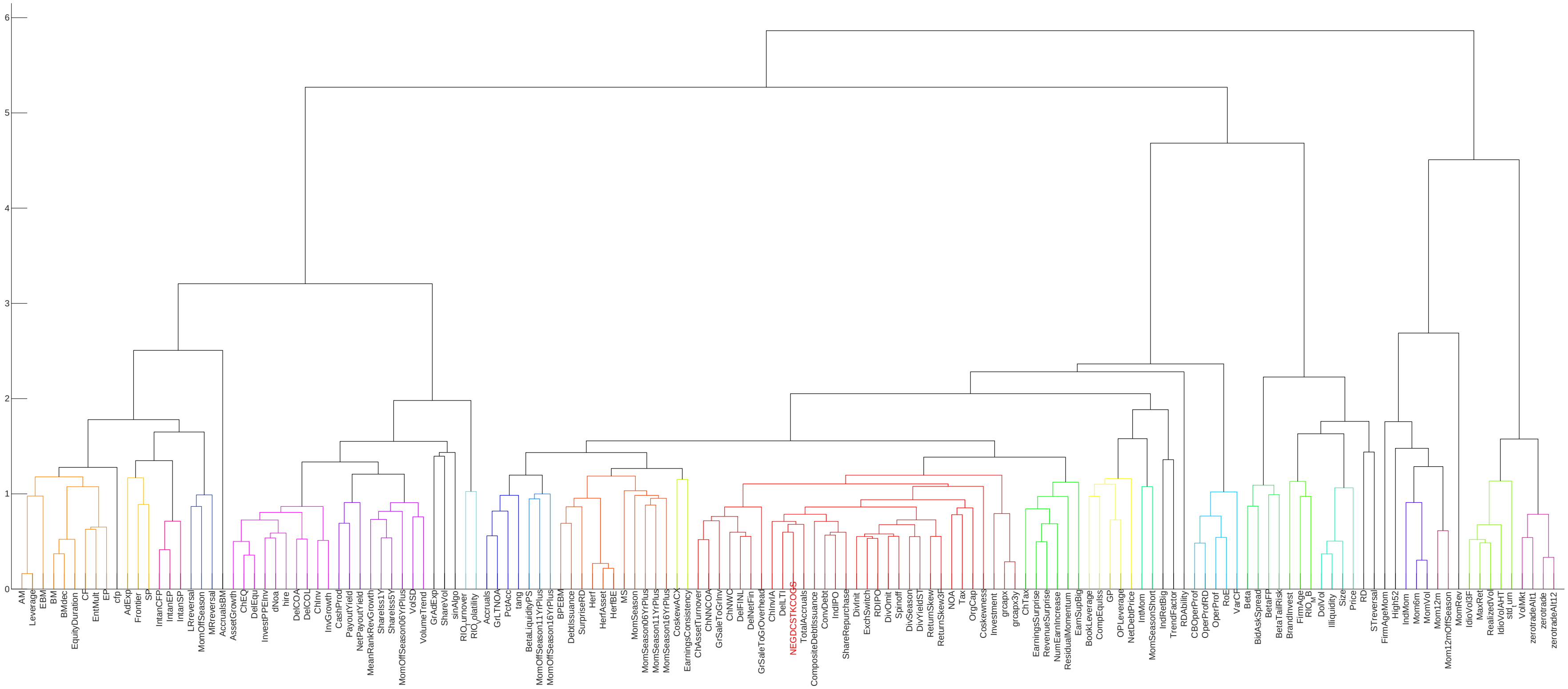

Figure 6: Agglomerative hierarchical cluster plot

This figure plots an agglomerative hierarchical cluster plot using Ward's minimum method and a maximum of 10 clusters.

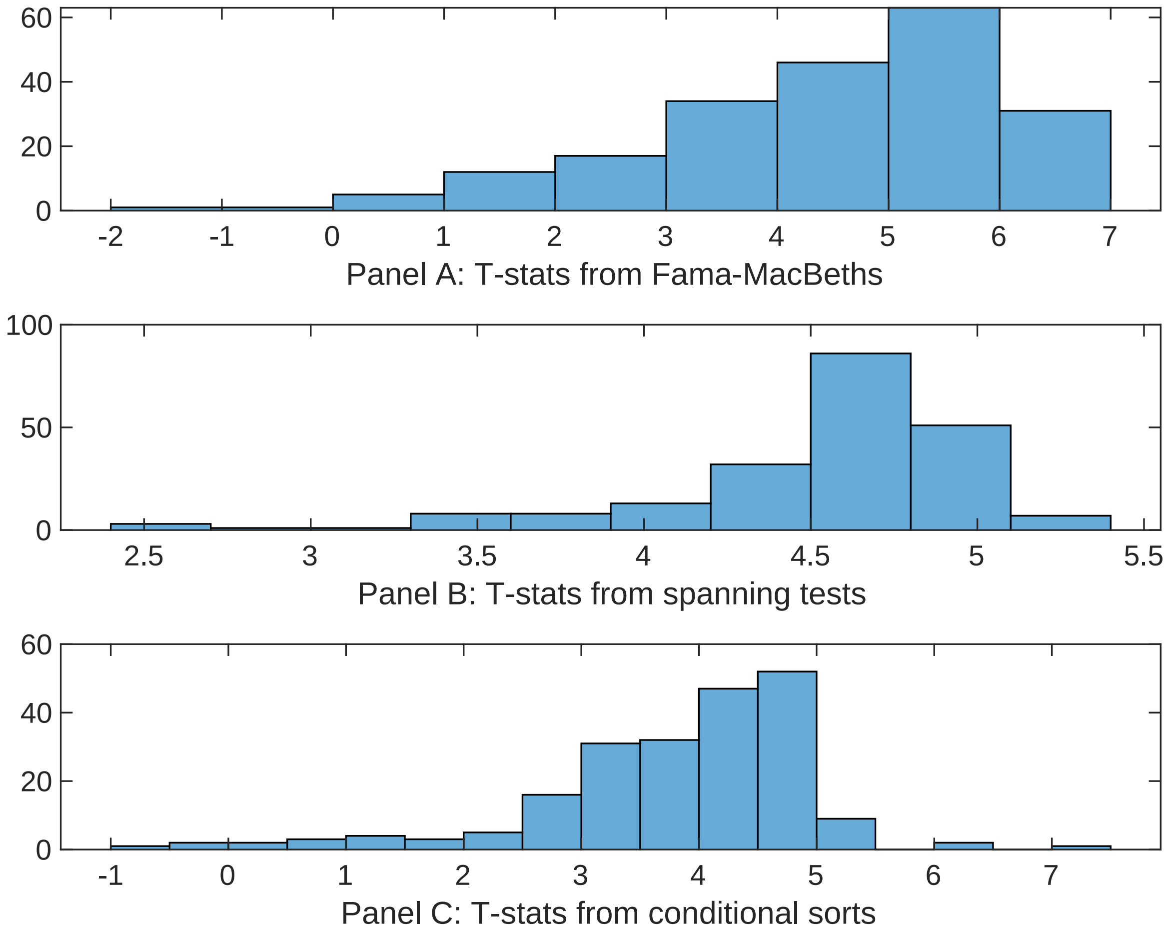

Figure 7: Distribution of t-stats on conditioning strategies
This figure plots histograms of t-statistics for predictability tests of IER conditioning on each of the 210 filtered anomaly signals one at a time. Panel A reports t-statistics on β_{IER} from Fama-MacBeth regressions of the form $r_{i,t} = \alpha + \beta_{IER} IER_{i,t} + \beta_X X_{i,t} + \epsilon_{i,t}$, where X stands for one of the 210 filtered anomaly signals at a time. Panel B plots t-statistics on α from spanning tests of the form: $r_{IER,t} = \alpha + \beta r_{X,t} + \epsilon_t$, where $r_{X,t}$ stands for the returns to one of the 210 filtered anomaly trading strategies at a time. The strategies employed in the spanning tests are constructed using quintile sorts, value-weighting, and NYSE breakpoints. Panel C plots t-statistics on the average returns to strategies constructed by conditional double sorts. In each month, we sort stocks into quintiles based one of the 210 filtered anomaly signals at a time. Then, within each quintile, we sort stocks into quintiles based on IER. Stocks are finally grouped into five IER portfolios by combining stocks within each anomaly sorting portfolio. The panel plots the t-statistics on the average returns of these conditional double-sorted IER trading strategies conditioned on each of the 210 filtered anomalies.

Table 4: Fama-MacBeths controlling for most closely related anomalies
This table presents Fama-MacBeth results of returns on IER. and the six most closely related anomalies. The regressions take the following form: $r_{i,t} = \alpha + \beta_{IER} IER_{i,t} + \sum_{k=1}^{s} ix\beta_{X_k} X_{i,t}^{k} + \epsilon_{i,t}$. The six most closely related anomalies, X, are Share issuance (1 year), Growth in book equity, Net Payout Yield, Share issuance (5 year), Change in equity to assets, Asset growth. These anomalies were picked as those with the highest combined rank where the ranks are based on the absolute value of the Spearman correlations in Panel B of Figure 5 and the R^2 from the spanning tests in Figure 7, Panel B. The sample period is 196606 to 202306.

Intercept	0.13	0.18	0.12	0.13	0.13	0.14	0.13
	[5.71]	[7.40]	[5.25]	[6.06]	[5.65]	[6.10]	[5.26]
IER	0.21	0.19	0.17	0.19	0.20	0.16	0.14
	[5.59]	[5.11]	[3.76]	[4.57]	[5.43]	[4.46]	[2.85]
Anomaly 1	0.26						0.99
	[5.74]						[2.36]
Anomaly 2		0.48					-0.17
		[4.37]					[-0.11]
Anomaly 3			0.27				0.22
			[2.37]				[2.05]
Anomaly 4				0.38			0.33
				[4.40]			[0.38]
Anomaly 5					0.15		-0.12
					[4.17]		[-0.21]
Anomaly 6						0.10	0.68
						[8.76]	[6.50]
# months	679	684	679	679	684	684	679
$\bar{R}^2(\%)$	0	0	1	0	0	0	0

Table 5: Spanning tests controlling for most closely related anomalies

This table presents spanning tests results of regressing returns to the IER trading strategy on trading strategies exploiting the six most closely related anomalies. The regressions take the following form: $r_t^{IER} = \alpha + \sum_{k=1}^{6} \beta_{X_k} r_t^{X_k} + \sum_{j=1}^{6} \beta_{f_j} r_t^{f_j} + \epsilon_t$, where X_k indicates each of the six most-closely related anomalies and f_j indicates the six factors from the Fama and French (2015) five-factor model augmented with the Carhart (1997) momentum factor. The six most closely related anomalies, X, are Share issuance (1 year), Growth in book equity, Net Payout Yield, Share issuance (5 year), Change in equity to assets, Asset growth. These anomalies were picked as those with the highest combined rank where the ranks are based on the absolute value of the Spearman correlations in Panel B of Figure 5 and the R^2 from the spanning tests in Figure 7, Panel B. The sample period is 196606 to 202306.

Intercept	0.18	0.20	0.20	0.17	0.22	0.21	0.16
	[2.51]	[2.85]	[2.71]	[2.38]	[3.02]	[2.82]	[2.39]
Anomaly 1	26.04						16.83
	[7.12]						[3.99]
Anomaly 2		34.85					36.31
		[8.89]					[6.37]
Anomaly 3			15.17				3.73
			[5.38]				[1.17]
Anomaly 4				13.65			0.36
				[3.57]			[0.09]
Anomaly 5					20.08		-8.65
					[5.20]		[-1.62]
Anomaly 6						7.13	-13.38
						[1.46]	[-2.66]
mkt	4.76	3.87	5.24	4.67	2.41	2.76	6.02
	[2.82]	[2.33]	[3.01]	[2.63]	[1.40]	[1.58]	[3.52]
smb	5.18	2.59	7.01	3.40	3.45	3.10	5.60
	[2.14]	[1.08]	[2.80]	[1.36]	[1.38]	[1.20]	[2.25]
hml	-2.56	-3.76	-5.02	-2.90	-2.22	0.08	-5.79
	[-0.78]	[-1.17]	[-1.43]	[-0.82]	[-0.66]	[0.02]	[-1.69]
rmw	1.44	11.72	1.48	7.48	11.89	9.78	3.57
	[0.41]	[3.62]	[0.40]	[2.18]	[3.52]	[2.87]	[0.93]
cma	17.88	-4.37	19.44	26.54	9.32	21.56	9.04
	[3.46]	[-0.72]	[3.62]	[5.18]	[1.47]	[2.79]	[1.22]
umd	2.79	2.58	4.39	3.23	3.55	3.15	2.05
	[1.68]	[1.57]	[2.60]	[1.90]	[2.08]	[1.81]	[1.25]
# months	680	684	680	680	684	684	680
$\bar{R}^2(\%)$	18	20	16	14	14	10	24

Panel A: Average rank

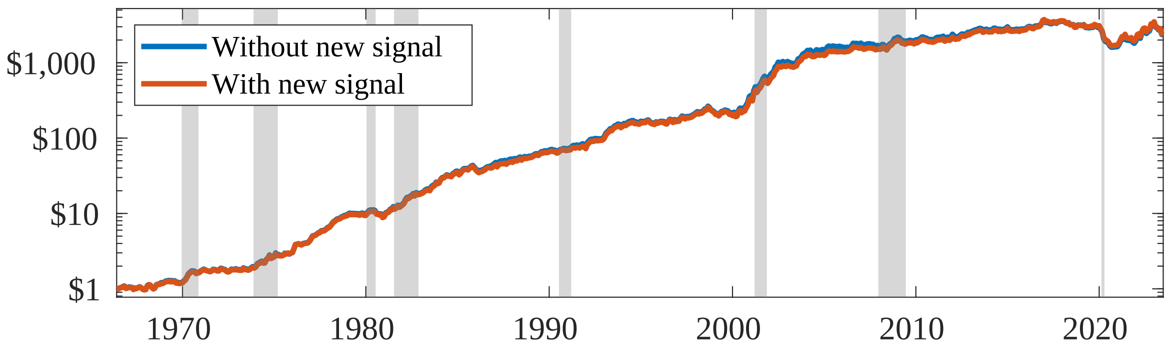

Figure 8: Combination strategy performance
This figure plots the growth of a $1 invested in trading strategies that combine multiple anomalies following Chen and Velikov (2022). In all panels, the blue solid lines indicate combination trading strategies that utilize 155 anomalies. The red solid lines indicate combination trading strategies that utilize the 155 anomalies as well as IER. Panel A shows results using "Average rank" as the combination method. See Section 7 for details on the combination methods.

References

Alan, Y., Gao, G. P., and Gaur, V. (2014). Does inventory productivity predict future stock returns? a retailing industry perspective. *Management Science*, 60(10):2416–2434.

Carhart, M. M. (1997). On persistence in mutual fund performance. *Journal of Finance*, 52:57–82.

Chen, A. and Velikov, M. (2022). Zeroing in on the expected returns of anomalies. *Journal of Financial and Quantitative Analysis*, Forthcoming.

Chen, A. Y. and Zimmermann, T. (2022). Open source cross-sectional asset pricing. *Critical Finance Review*, 27(2):207–264.

Chen, H., Frank, M. Z., and Wu, O. Q. (2005). The impact of operational efficiency on firm performance. *Journal of Financial Economics*, 78(3):563–593.

Cooper, M. J., Gulen, H., and Schill, M. J. (2008). Asset growth and the cross-section of stock returns. *Journal of Finance*, 63(4):1609–1651.

Detzel, A., Novy-Marx, R., and Velikov, M. (2022). Model comparison with transaction costs. *Journal of Finance, Forthcoming.*

Fama, E. F. and French, K. R. (1993). Common risk factors in the returns on stocks and bonds. *Journal of Financial Economics*, 33(1):3–56.

Fama, E. F. and French, K. R. (2015). A five-factor asset pricing model. *Journal of Financial Economics*, 116(1):1–22.

Fama, E. F. and French, K. R. (2018). Choosing factors. *Journal of Financial Economics*, 128(2):234–252.

Harvey, C. R., Liu, Y., and Zhu, H. (2016). ... and the cross-section of expected returns. *Review of Financial Studies*, 29(1):5–68.

Hirshleifer, D. and Teoh, S. H. (2003). Limited attention, information disclosure, and financial reporting. *Journal of Accounting and Economics*, 36:337–386.

Novy-Marx, R. and Velikov, M. (2016). A taxonomy of anomalies and their trading costs. *Review of Financial Studies*, 29(1):104–147.

Novy-Marx, R. and Velikov, M. (2023). Assaying anomalies. *Working paper.*

Sloan, R. G. (1996). Do stock prices fully reflect information in accruals and cash flows about future earnings? *The Accounting Review*, 71(3):289–315.

Titman, S., Wei, K. J., and Xie, F. (2004). Capital investments and stock returns. *Journal of Financial and Quantitative Analysis*, 39(4):677–700.